Complex light fields enter a new dimension: holographic modulation of polarization in addition to amplitude and phase

E. Otte*, C. Schlickriede, C. Alpmann, and C. Denz
Institute of Applied Physics, University of Muenster, Corrensstraße 2/4, 48149 Münster, Germany

ABSTRACT

We present a method to tailor not only amplitude and phase of a complex light field, but also the transverse states of polarization. Starting from the implementation of spatially inhomogeneous distributions of polarization, so called Poincaré beams, we realized a holographic optical technique that allows arbitrarily modulating the states of polarization by a single phase-only spatial light modulator (SLM). Moreover, the effective amplitude modulation of higher order beams performed by a phase-only SLM is shown. We will demonstrate the capabilities of our method ranging from the modulation of higher order Gaussian modes including desired polarization characteristics to the generation of polarization singularities at arbitrary points in the transverse plane of Poincaré beams.

Keywords: structured light, higher order modes, Laguerre-Gaussian beams, polarization, Poincaré beams, phase correction, holographic modulation

1. INTRODUCTION

Complex light fields with a spatially inhomogeneous distribution of polarization are of growing scientific interest [1]. So called Poincaré beams [2] especially with polarization singularities as L-Lines, C-Lines, V-Points and C-Points appearing in their transverse plane reach the state of a highly investigated topic [3, 4]. Typically, Poincaré beams and polarization singularities are generated exploiting birefringence [2, 5], q-plates [6], or by interferometric methods [7]. However, these methods do neither allow an arbitrary transverse location of polarization singularities nor a full combination of amplitude, phase, and polarization modulation of the complete transverse plane.

Our holography-based method is not only capable of tailoring complex light fields [8] by amplitude and phase modulation but also allows arbitrarily modulating the states of polarization such that Poincaré beams with polarization singularities can be created. In order to perform amplitude and phase modulation SLMs are a widely used optical component [8]. Our experimental system employs a single reflective phase-only SLM operating in a split-screen-mode for the modulation of amplitude, phase and, in addition to that, of polarization. To use the SLM effectively, different correction methods are necessary: The active LC-layer (LC: liquid crystal) of the SLM used for modulation exhibits considerable differences in thickness – this means by using the SLM as a reflective optical component, undesired disturbances in the beams' spatial phase distribution are caused [10]. Different methods exist, which were used to correct undesired effects as e.g. a blurred spot of a focused beam due to the disturbance in phase. An example is the determination of an elliptical correction mask based on an assumed astigmatism [11]. The parameters of the correction mask are found experimentally by trial and error parameters in this case. Another example is the usage of Zernike polynomials in order to correct common aberrations of the beam's focus and occurring astigmatism [12]. These methods were mainly created in order to optimize the application of SLMs in optical micromanipulation by optical tweezers, where the trapping stiffness depends on the fidelity of the focused beam (spot sharpness) used for optical trapping of microparticles [12].

We will combine different modulation methods including corrections to achieve on the one hand the theoretically expected amplitude and phase distribution of complex beams, as e.g. higher order Laguerre-Gaussian beams, experimentally and on the other hand the effective modulation of arbitrary spatial distributions of polarization in order to create Poincaré beams. In section 2 we will discuss the amplitude and phase modulation performed by a reflective phase-only SLM implementing a proposed correction method based on [13] used to enhance the quality of the spatial accuracy of modulation. The utilization of the SLM for the dynamic polarization modulation and the corresponding correction method is described in section 3.

*eileen.otte@uni-muenster.de; phone 0049 251 83 39116

Moreover, we will demonstrate the capabilities of our methods ranging from the effective modulation of higher order Gaussian modes including desired polarization characteristics to the generation of polarization singularities at arbitrary points in the transverse plane of Poincaré beams in section 4. The properties of these beams can be applied in optical micromanipulation, where polarization properties are used to align anisotropic particles [14]. Additionally, application in information technology for advanced information encoding is possible [15, 16].

2. AMPLITUDE- AND PHASE MODULATION

2.1 Phase-only spatial light modulator for the modulation of complex light fields

Amplitude and phase modulation for the creation of complex light fields as higher order Gaussian beams is usually performed by the use of SLMs [9]. If a phase-only SLM is utilized for the modulation, an advanced technique is necessary in order to modulate phase as well as amplitude simultaneously and independently: The ansatz for this method was described by Davis *et al.* in 1999 [17] based on weighting a blazed grating given on the SLM by the desired field amplitude. The complex light field E, which is supposed to be modulated, can be written as

$$E = A \cdot \exp(\mathrm{i}\phi), \tag{1}$$

whereby $A \in [0, 1]$ describes the normalized amplitude and $\phi \in [0, 2\pi)$ the phase. The idea in [17] is to encode the light field as a phase function

$$T = \exp(\mathrm{i}A\phi), \tag{2}$$

which can be shown in the form of a mixed Fourier-Taylor-function

$$T = \sum_{n=-\infty}^{\infty} T_n \exp(\mathrm{i}n\phi) \tag{3}$$

with the coefficients

$$T_n = \exp(-\mathrm{i}[n - A]\pi) \cdot \mathrm{sinc}(n - A). \tag{4}$$

If we choose to use just the first diffraction order with $n = 1$, we obtain a modulation with a phase term $\exp(-\mathrm{i}[1 - A]\pi)$ in addition to the desired phase of (1). Moreover, the amplitude's information can be found in the sinc-function of T_1, but is just approximately reconstructed by $|T_1| = \mathrm{sinc}(1 - A)$. In order to get the desired field distribution (1), the achieved amplitude and phase need to be corrected. The additional phase term in T_1 can be eliminated easily by multiplying by its complex conjugate. The generation of the desired amplitude is slightly more elaborate: With the help of a look-up table (LUT) the values of the inverse sinc-function can be determined.

To separate the first diffraction order T_1 spatially from the others, a blazed grating is added on the SLM created by the modulo 2π of a linear phase ramp. This linear phase in the image plane of the SLM causes a spatial separation of the orders in the Fourier plane of the SLM's surface [18]. In the experimental setup sketched in figure 1 a), a Fourier filter (A: aperture) is used to only pass the first diffraction order due to the spatial separation.

We can conclude that for the generation of complex light fields modulated in amplitude and phase by the use of a phase-only SLM, we need to apply a phase hologram given by

$$\Theta_{\mathrm{H}} = A_{\mathrm{LUT}} \cdot (\phi + \phi_L - A_{\mathrm{LUT}} \cdot \pi)\,. \tag{5}$$

A_{LUT} describes the amplitude using the look-up table (LUT), which is needed to be applied in order to achieve the desired amplitude A instead of the sinc-term in T_1. Moreover, ϕ is the phase of the desired complex light field and ϕ_L depicts the linear phase ramp used to separate the orders of T_n.

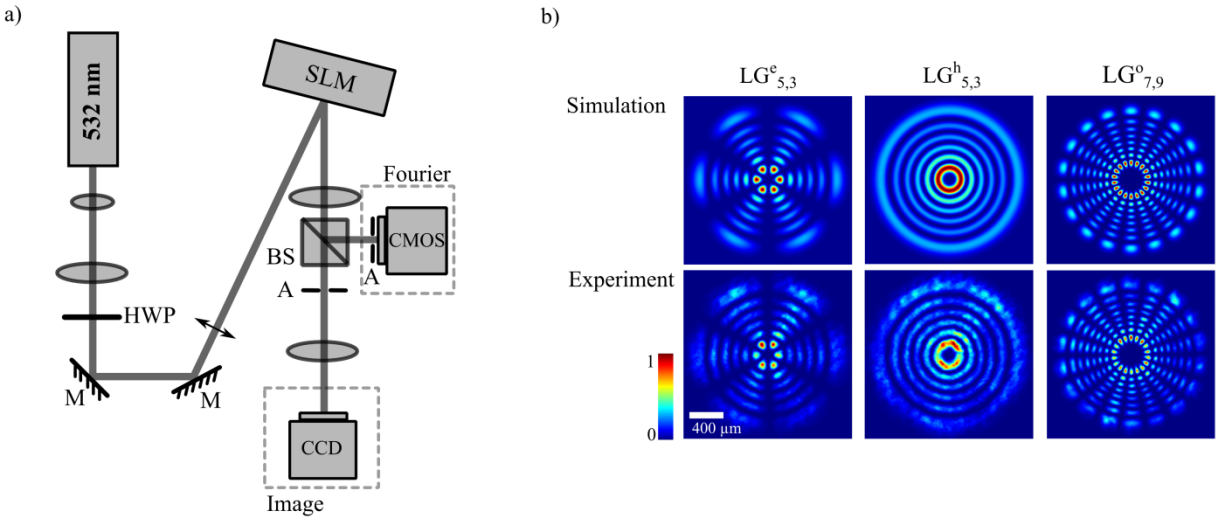

Figure 1. a) Schematic of the experimental setup for amplitude and phase modulation – M: mirror, HWP: half wave plate, SLM: spatial light modulator, BS: beam splitter, A: aperture, CCD/ CMOS: CCD/ CMOS camera, Image: image plane of SLM, Fourier: Fourier plane of SLM. b) Comparison of theoretic (upper row) and experimental (lower row) results of higher order Laguerre-Gaussian beams modulated in amplitude and phase by the phase-only SLM – LG^e/ LG^h/ LG^o:even/ helical/ odd Laguerre-Gaussian beam.

This method and setup facilitates the creation of arbitrary light fields modulated in amplitude and phase. Examples of higher order Laguerre-Gaussian beams (LG^e/ LG^h/ LG^o: even/ helical/ odd Laguerre-Gaussian beam) created by our setup are shown in figure 1 b), while a comparison between simulations (upper row) and experimentally generated beams (lower row) is shown: the intensity distribution of the higher order modes match the theoretical expectations (simulations) if the applied phase hologram corresponds to the form of Θ_H described in equation (5).

2.2 Phase correction of SLM-modulated beams

As already mentioned in section 1, spatial light modulators may cause discrepancies between theoretical expected and the experimentally achieved phase distribution of the desired complex light field due to the imperfect transverse phase flatness of the phase-only SLM [10]. In the setup shown in figure 1 a) the reflective phase-only SLM was used to modulate amplitude and phase as described in section 2.1.

Different methods exist to correct this phase inhomogeneity, for example the determination of an elliptical correction mask based on an assumed astigmatism [11] or the use of Zernike polynomials [12]. In contrast, we developed and implemented a correction method which is based on an *in situ* spot correction in the Fourier plane (correction plane, see fig. 1 a)) of the light field [12]. In this case, the modulator's surface, including the linear phase ramp ϕ_L (see sec. 2.1), and thus the modulated light field is divided into quadratic modes (e.g. 60x60 pixels). Optimal focusing and thus a sharp spot in the Fourier plane is achieved if all the modes meet at a selected point in space with the same phase; maximum intensity in this point is reached for constructive interference of all modes. For the correction of phase deviations caused by optical components as the SLM and resulting in a blurred spot in the Fourier plane, one mode is chosen to be the reference mode, which is supposed to interfere with a single mode of the other signal modes in the respective plane. The modes can be turned on and off independently. By measuring the intensity at the focal point while shifting the signal mode under consideration in phase, the optimal phase shift is determined for which the intensity signal is maximal. In this case, reference and tested signal mode have the same phase. This process is repeated for each signal mode, whereby the optimal phase shift is supposed to be used as corrective phase value per mode, respectively.

As a result, a phase correction pattern is created, and subsequently used on the SLM's surface to result in an ideal focal spot in the Fourier plane. The complete correction process is sketched in figure 2: subfigure a) shows the blazed grating used to separate the orders spatially for the case of amplitude and phase modulation by a phase-only SLM, b) depicts the resulting blurred spot in the Fourier plane; c) illustrates the method of interfering modes resulting in an interference

pattern in the correction plane (d)); e) depicts the phase correction pattern plus blazed grating utilized as the hologram on the SLM and f) the achieved focal spot in the Fourier plane, while g) illustrates the determined phase correction pattern with 16 times 18 modes (each mode 60x60 pixels/ 480x480 µm on SLM).

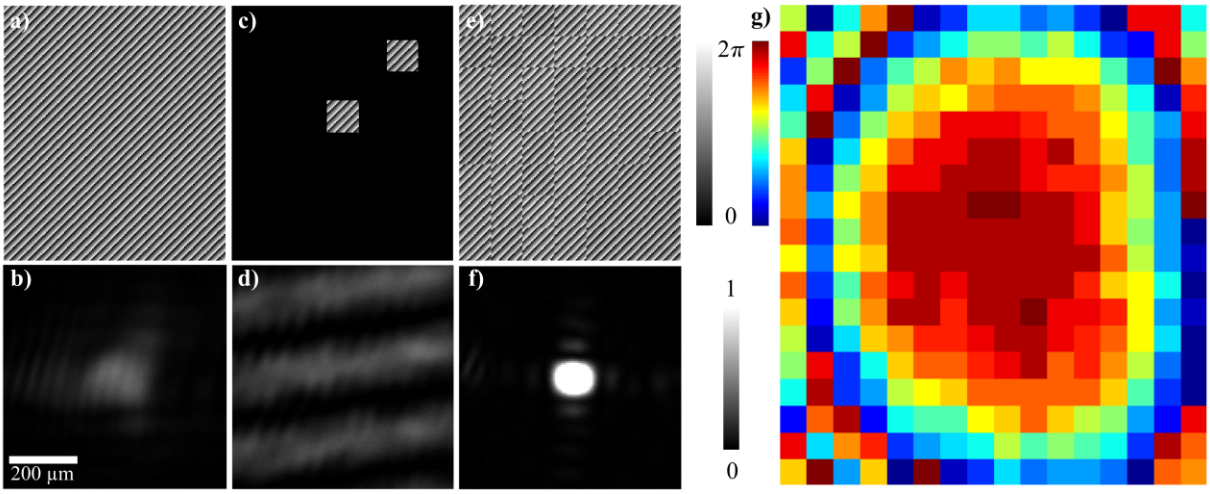

Figure 2. Method of phase correction: a) An uncorrected blazed grating causes a blurred spot in the Fourier plane shown in b) due to spatial inhomogeneities of the SLM. c) By the interference of two spatial modes (reference and signal mode) in the Fourier plane an interference pattern depicted in d) is created. The maximum intensity in the focal point is adjusted by shifting the regarded signal mode in phase – the corresponding phase shift of all signal modes is used as phase correction pattern. e) A superposition of the blazed grating with the determined phase correction pattern results in a sharp spot (f)) in the Fourier plane, thus, the beam's phase front is corrected. The determined phase correction pattern for the used SLM is shown in g).

The measured phase correction pattern has a rough pixel structure – this structure causes a homogeneous phase distribution but disturbances in the intensity structure in the image plane of the SLM. For the purpose of minimizing undesired effects, it is possible to reduce the modes' size considering that the intensity of the interference pattern meets the requirement of the phase correction method. Another possibility in order to minimize the disturbances in the image plane is to find a continuous fit for the measured phase correction. Figure 3 shows a comparison with respect to the measurable intensity distribution in the image and Fourier plane for the case without phase correction (fig. 3a)), of the determined 16x18-modes phase correction pattern (fig. 3b)) and, finally, of a continuous, elliptical fit of the measured correction (fig. 3c)) for the used SLM. Obviously, the pixel structure results in the expected Gaussian distribution in the Fourier plane, whereas the image plane reveals clear disturbances if we use neither an amplitude nor a phase modulation. In contrast, the continuous, elliptical structure results in a minimally worse profile in the Fourier plane, while the image plane shows a distinctly better intensity distribution. Moreover, figure 3 also includes a comparison of both correction methods for the case of modulating a self-similar [19], higher order Laguerre-Gaussian beam ($LG^{e}_{7,9}$) by applying the modulation method described in section 2.1. Although both correction methods reveal a clear optimization with respect to the case without correction, minor differences can be observed. We use the continuous, elliptical phase correction in order to achieve good results in the image and also comparatively good results in the Fourier plane.

If the modulation is performed as explained in section 2.1 and the correction of phase is considered, good results for complex light fields modulated in amplitude and phase by a single phase-only SLM will be obtained, which match the corresponding theory.

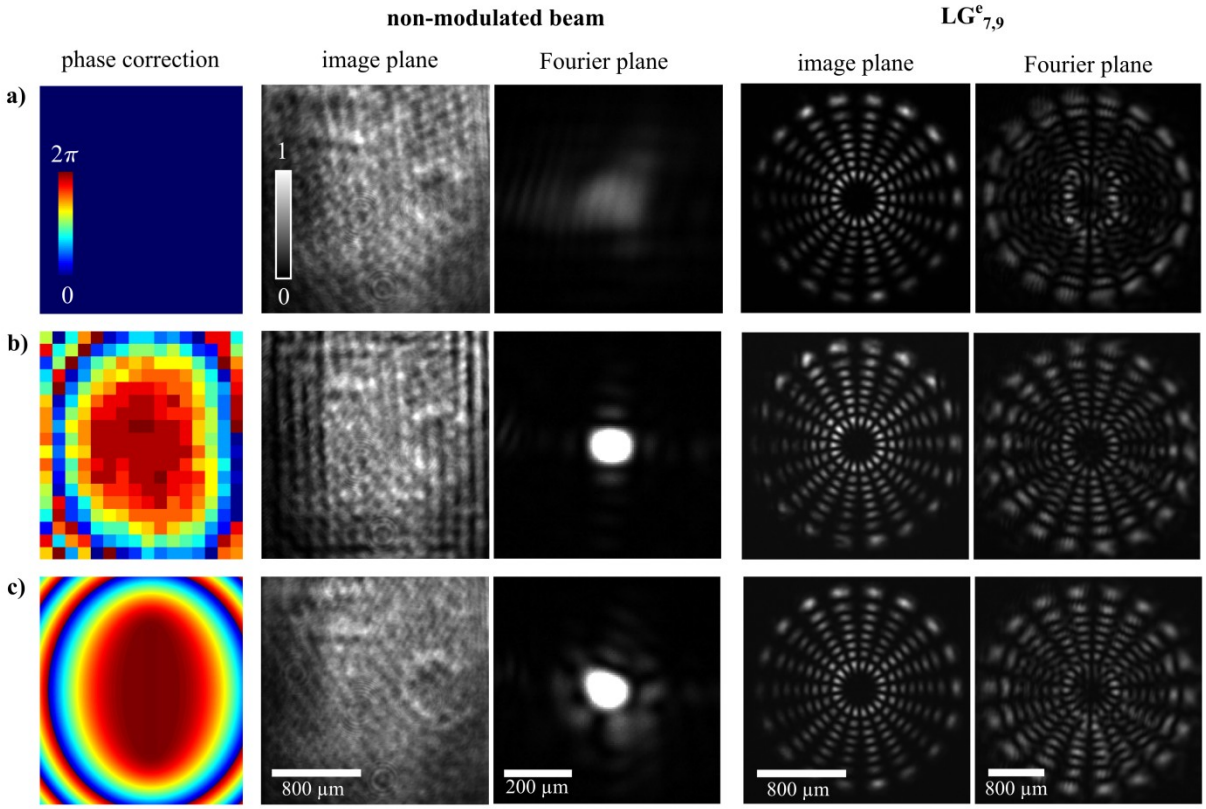

Figure 3. Comparison of the intensity distribution in the image and Fourier plane for a non-modulated beam and a modulated even Laguerre-Gaussian beam ($LG^{e}_{7,9}$) for different phase correction patterns, respectively: a) shows the results achieved by the utilization of no phase correction, b) of the experimentally determined phase correction pattern (rough pixel structure) and c) of the continuous elliptical fit of the measured correction pattern. Without any correction, not only the intensity distribution in the image plane, but also in the Fourier plane is disturbed. b) shows the enhancement achieved by the usage of a phase correction pattern especially in the Fourier plane, while the intensity in the image plane includes undesired disturbances. In contrast to this c) reveals very good results in the image plane, while the intensity distribution in Fourier plane is slightly disturbed. Regarding the further purpose of the investigated setup the correction pattern of c) gives the best results.

3. DYNAMIC POLARIZATION MODULATION

Besides the generation of complex light fields modulated in amplitude and phase, the phase-only SLM (parallel aligned nematic-liquid crystals) can be a key component for the dynamic polarization modulation of light fields in order to create a spatially inhomogeneous distribution of transverse states of polarization [21]. For this purpose, the spatial polarization modulator (SPM) is utilized, which will be described in the following section 3.1.

3.1 Spatial polarization modulator

For the generation of an arbitrary spatial distribution of states of polarization the phase-only SLM is used in a configuration in between two quarter wave plates (QWP). These three optical components represent the spatial polarization modulator (SPM) as sketched in figure 4 a) [20, 21].

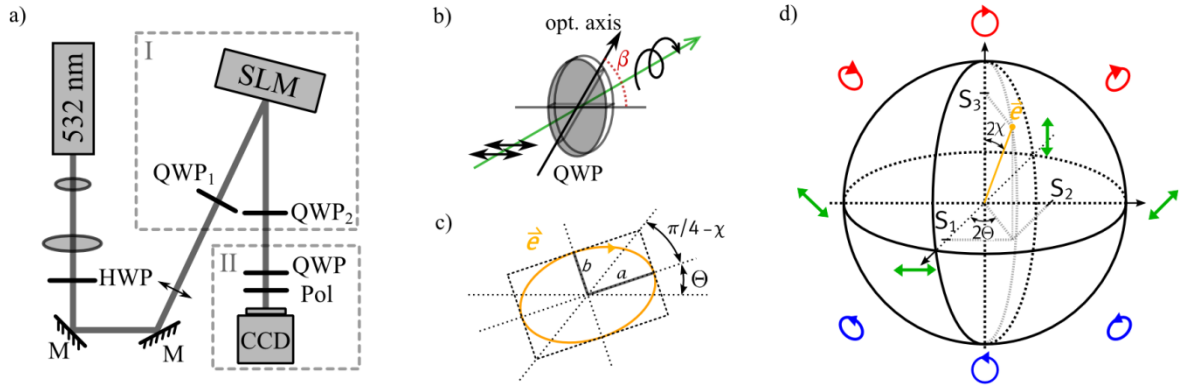

Figure 4. Spatial modulation of polarization. a) shows the outline of the experimental setup for the polarization modulation – I: spatial polarization modulator (SPM) consisting of two quarter wave plates (QWP) enclosing a spatial light modulator (SLM), II: polarization measurement setup composed of a rotatable quarter wave plate and a polarizer (Pol) in front of a CCD camera (CCD). The input polarization supposed to be modulated by the SPM is horizontally linear and created by a half wave plate (HWP). The angles of the SPM's QWPs are chosen to be $\beta_1 = -45°$ and $\beta_2 = 90°$ regarding the input polarization (see b)), while the phase shift $\Delta\phi_{SLM}$ introduced by the SLM is variable. Subfigure c) illustrates the parameters of the polarization ellipses and d) demonstrate the Poincaré sphere spanned by the Stokes parameters S_1, S_2 and S_3 and used to visualize states of polarization, e.g. $\vec{e}$. Right/ left elliptical states of polarization are indicated as red/ blue ellipses, while linearly polarized states are colored green.

Corresponding to Jones calculus, transverse polarization is defined as $\vec{e} = (e_x, e_y)$. Polarization components oriented in the $(1, 0)$-direction and, thus, parallel to the horizontally aligned liquid crystals of the phase-only SLM, can be shifted in phase, while components orthogonal to the crystals ($(0, 1)$-direction) cannot be altered by the SLM [22]. Thus, the SLM can introduce a phase shift $\Delta\phi_{SLM}$ between horizontally (e_x) and vertically (e_y) polarized components. In the case under consideration, the first quarter wave plate (QWP_1) in front of the SLM is used to determine the amplitude ratio between horizontally and vertically polarized light reaching the SLM: After expanding the laser beam by two lenses, the beam is horizontally, linearly polarized by a half wave plate (HWP). Depending on the angle β_1 between the fast axis of QWP_1 and the linear input polarization (see fig. 4 b)), the input polarization is transformed into elliptic polarization with β_1-dependent ellipticity. We choose $\beta_1 = -45°$, so that circular polarized light is generated behind QWP_1. By the additional use of the second quarter wave plate (QWP_2) the orthogonal polarization components with the introduced phase shift are recombined depending on the angle β_2 enclosed by the fast axis of QWP_2 and the incoming state of polarization in front of the SPM. For the second quarter wave plate $\beta_1 = 90°$ is chosen.
The phase shift $\Delta\phi_{SLM}$ introduced by the phase-only SLM represents a degree of freedom which can vary between zero and 2π, while each value leads to a different state of polarization if $\beta_1 = -45°$ and $\beta_2 = 90°$. The opportunity to spatially (pixelwise) vary the phase shift $\Delta\phi_{SLM}(x, y)$ of the SLM provides the feature of spatially varying the states of polarization with the help of the SPM [21].

Usually, states of polarization are represented by the Poincaré sphere, which is spanned by the Stokes parameters S_1, S_2 and S_3. Completely polarized states can be found on the unit sphere's surface, right elliptical states of polarization (REP) are positioned on the upper hemisphere, left elliptical states (LEP) on the lower hemisphere. Consequently, the equator includes all linearly polarized states, north and south pole contain right and left circular polarized states (RCP, LCP), respectively. Each point on the Poincaré sphere can be defined by the angles Θ and χ, which are linked to the polarization ellipse corresponding to this point on the sphere (see fig. 4 c), d)): Θ defines the orientation, χ the opening angle and thus the ellipticity of the polarization ellipse.
If we choose to have a fixed set of angles $\beta_1 = -45°$ and $\beta_2 = 90°$ for QWP_1 and QWP_2, and a variable phase shift $\Delta\phi_{SLM}(x, y)$, polarization states, which are accessible simultaneously in the transverse plane of a beam modulated by the SPM, lay on a circular ring on the Poincaré sphere [21]: all accessible states are located on the circle in the S_2-S_3-plane, while $S_1 = 0$ $(\forall\, x, y)$. Consequently, by choosing a suitable phase hologram $\Delta\phi_{SLM}(x, y)$ for the SLM, beams with spatially varying states of polarization can be formed, i.e. Poincaré beams [2] can be created. Experimental results with regard to the generation of different kinds of Poincaré beams will be shown in section 4.

3.2 Polarization correction method

In section 2.2 we discussed how to handle an imperfect phase homogeneity in the transverse plane of beams introduced by the phase-only SLM. This prevents disturbances in the case of modulating amplitude and phase for the creation of complex light fields as higher order Laguerre-Gaussian beams. Because disturbances in the phase distribution caused by the SLM will also be transferred into disturbances in the desired spatial modulation of polarization realized by the SPM, an appropriate correction method needs to be adapted for this case.

Figure 5 a) visualizes the measured polarization distribution in the transverse plane of a Gaussian beam, while $\beta_1 = -45°$, $\beta_2 = 90°$ and the SLM carry a value of $\Delta\phi_{\mathrm{SLM}} = 0$ for the whole surface. As already mentioned, the accessible states of polarization lay on the ring in the S_2-S_3-plane of the Poincaré sphere as shown in figure 5 a). The measurement of Stokes parameters is performed as described in [23] with the help of a rotatable QWP and a fixed polarizer in front of a CCD-camera in the image plane of the SLM while the intensity is determined in each pixel (see fig. 4a), part II). Obviously, even if the phase shift $\Delta\phi_{\mathrm{SLM}}(x, y)$ introduced by the SLM was chosen to be zero for all *x* and *y*, the states of polarization vary over the transverse plane. According to theoretical calculations performed via Jones calculus, the transverse plane should just include $-45°$-linearly polarized states, i.e. a Stokes vector $\vec{S} = (S_0, S_1, S_2, S_3) = (1, 0, -1, 0)$, orientation angle $\Theta = -\pi/4$ and opening angle of polarization ellipses $\tan(\chi) = 0$ for every spatial position (see bottom left corners in a)). Nevertheless, the measurement offers states with REP ($S_3 > 0$) varying spatially in ellipticity (especially visible in $\tan(\chi)$) and even varying in orientation (especially obvious in Θ).

For the correction of the inhomogeneous distribution of polarization, we calculated the position-dependent phase shift $\delta_1(x, y)$ between horizontally and vertically polarized components with regard to our measurement results, which is given by

$$\delta_1(x, y) = \arctan\left(\frac{S_3(x,y)}{S_2(x,y)}\right), \in [-\pi/2, \pi/2] \tag{6}$$

This calculation results in the first step of our correction for the polarization modulation: by the use of $\mathrm{mod}(-\delta_1(x, y), \pi)$ as a phase correction hologram on the SLM shown in figure 5 b), the transverse distribution of polarization becomes more homogeneous as being especially visible in S_2, $\tan(\chi)$ and Θ, respectively. The horizontal components reflected from the SLM are shifted in phase according to the correction pattern, which is supposed to eliminate the undesired phase shift between horizontal and vertical polarization components. Now, the orientation Θ of polarization ellipses is correct, moreover, the ellipticity χ is considerably smaller than before.

Despite the achieved enhancement, disturbances can still be found in the spatial polarization distribution. In order to enhance the distribution further, the described process is repeated so that an additional correction pattern $\delta_2(x, y)$ is calculated from the measurement performed utilizing the correction $\delta_1(x, y)$ (for the SLM we use $\mathrm{mod}(-\delta_1(x, y), \pi)$). This results in the overall correction pattern

$$\delta_{corr}(x, y) = \mathrm{mod}[-\delta_1(x, y) - \delta_2(x, y), \pi]\,. \tag{7}$$

By the use of this correction pattern, the spatial distribution of states of polarization becomes nearly homogeneous and mostly $-45°$-linearly polarized (see fig. 6 c)) as theoretically expected. If further correction is desired or needed, the procedure can be repeated again.

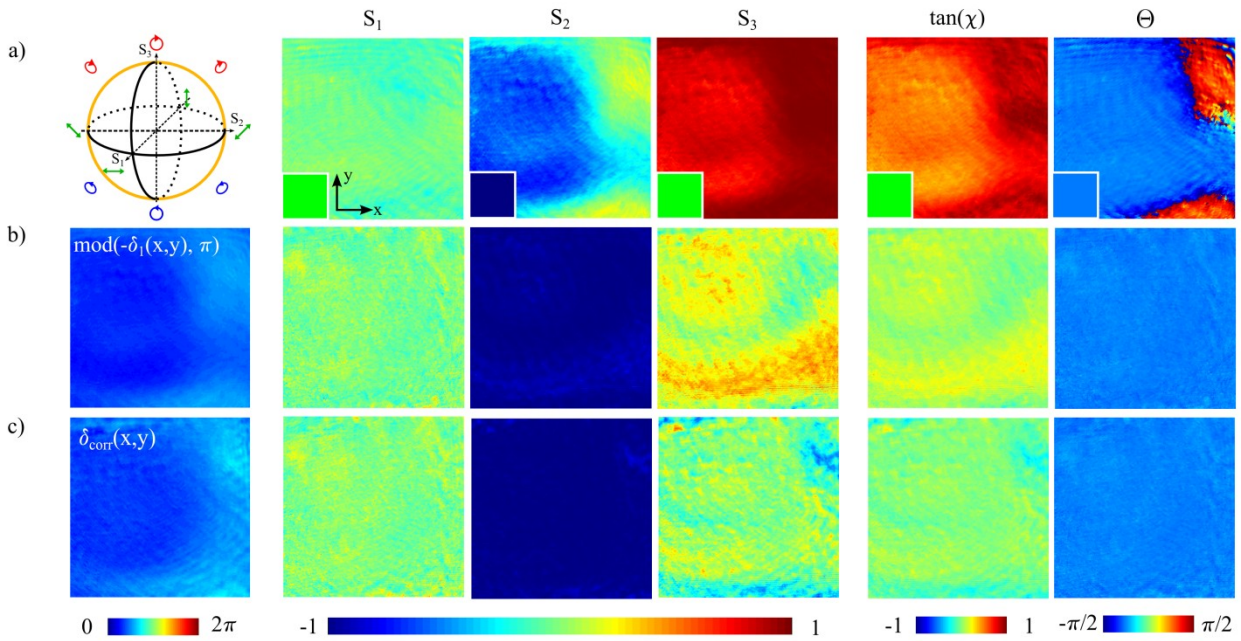

Figure 5. Determination of the correction pattern for the polarization modulation by the SPM: The QWPs' angles are fixed at $\beta_1 = -45°$ and $\beta_2 = 90°$, so that all polarization states located on the ring in the S_2-S_3-plane of the Poincaré sphere are reachable by changing $\Delta\phi_{SLM}$ (see a), left). a) shows the measured Stokes parameters S_1, S_2 and S_3 and ellipses properties $\tan\chi$ (opening angle) and Θ (orientation) whose spatial distribution is inhomogeneous if $\Delta\phi_{SLM}(x,y) = 0$ is chosen for all x and y, thus, no correction pattern is used. In the bottom left corner the theoretically expected value is shown color-coded for each measured parameter. b) visualizes the same measured parameters if a first correction pattern $\mathrm{mod}(-\delta_1(x,y),\pi)$ for the SLM is utilized. It is determined by the Stokes parameters of a). The Stokes parameters of b) are used further for the determination of the final polarization modulation correction pattern $\delta_{corr}(x,y)$. If this pattern is applied, the parameters are nearly spatially homogeneous compared to the parameters measured without any correction in a) and carry the correct values compared to the theoretically expected ones (see bottom left corners in a)).

4. REALIZATIONS OF POINCARÉ BEAMS WITH SIMULTANEOUS AMPLITUDE, PHASE AND POLARIZATION MODULATION

4.1 Generation method of simultaneous amplitude, phase and polarization modulation

The spatial polarization modulator (SPM) described in section 3 enables the creation of complex light fields with a spatially varying distribution of polarization [21], such that Poincaré beams [2] can be created. In addition, we extend our technique to additional amplitude and phase modulation implemented by a single reflective phase-only SLM. For this purpose, a full HD SLM is used in a split-screen-mode: The first half of the SLM modulates amplitude and phase, as explained in section 2, the second half enclosed by two quarter wave plates creates the desired spatial distribution of polarization states by acting as a SPM, as described in section 3.

Figure 6 shows an outline of the combined experimental setup (a)) and the modulation method (b) - e)). Subfigure c) indicates the light field generated behind the first half of the SLM if the hologram in b) (left) is used: the beam is modulated in amplitude and phase ($LG^e_{5,3}$; grayscale image of the simulated intensity distribution is shown in the background), but still carrys a spatially homogeneous distribution of polarization visualized by horizontal, green arrows symbolizing horizontally linear polarized states. By a 4-f-setup the first half of the SLM and thus the light field modulated in amplitude and phase is imaged on the second half of the SLM in order to modulate the light field's polarization. By the choice of the phase hologram for the second half (see fig. 6 b), right), which is equal to the polarization modulation hologram, the desired spatial distribution of polarization can be achieved as indicated in figure 6 d) showing the complex light field after passing the SPM: each wing of the Laguerre-Gaussian beam modulated by the first half of the SLM ($LG^e_{5,3}$; grayscale image of the simulated intensity distribution is shown in the background) got its own state of polarization by the use of the SPM (red/ blue ellipses: right/ left elliptical polarization states). Figure 6 e)

shows the chosen states for the modulation of polarization, which are located on the ring in the S_2-S_3-plane. Each point belongs to a certain phase shift $\Delta\phi_{SLM}$ and, thus, to one of the wings of the complex beam, while the angles of the QWPs are given by $\beta_1 = -45°$ and $\beta_2 = 90°$.
In order to investigate the generated complex beams, another 4-f-setup is used to image the second half of the SLM on the camera located in the conjugated plane of the SLM (image plane); moreover, observing in its Fourier plane is possible, too.

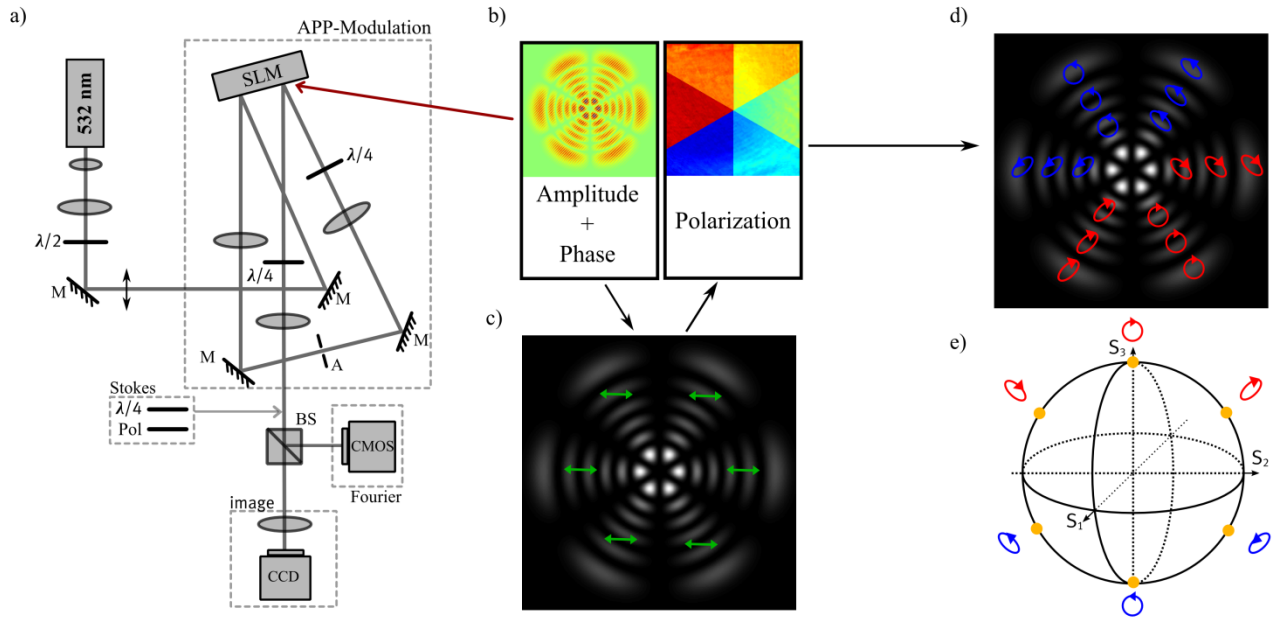

Figure 6. Outline of the experimental setup and method used for amplitude, phase and polarization modulation (APP-Modulation): the reflective, phase-only SLM is used in split-sceen-mode, so that the first half can be utilized to modulate amplitude and phase (see sec. 2), the second half enclosed by two quarter wave plates ($\lambda/4$) creates the desired polarization distribution by acting as a SPM (see sec. 3), as indicated in b) - d). b) shows the used modulation holograms including the correction holograms, while c) indicates the light field achieved after the first half of the SLM – in the shown case an even Laguerre-Gaussian beam ($LG^e_{5,3}$; grayscale image of the simulated intensity distribution is shown in the background) containing only horizontally linear polarized states (green arrows). After passing the SPM a complex light field modulated in amplitude, phase and polarization is realized as depicted in d): each wing of the $LG^e_{5,3}$-beam got its own state of polarization (red/ blue ellipses indicating right/ left elliptical polarization states). In e) the chosen states for the polarization modulation are shown on the Poincaré sphere. In order to determine the states of polarization, a measurement system consisting of a rotatable quarter wave plate and a polarizer (Pol) can be included into the setup, while the complex light field can be observed in the image or the Fourier plane of the SLM. ($\lambda/2$: half wave plate, M: mirror, A: aperture, BS: beam splitter, CCD/ CMOS: CCD/ CMOS camera)

The camera in the Fourier plane is utilized to determine the phase correction pattern for the case of amplitude and phase modulation as described in section 2.2. For this measurement the second half of the SLM is chosen to be zero (just reflection, no modulation) and the QWPs of the SPM are removed. Note that in this case the phase correction pattern is determined to be a hologram on the first half of the SLM, while it corrects the uneven surface of the first and the second half: undesired phase shifts caused by any optical component following the first half of the SLM are corrected by measuring the interference of modes in the Fourier plane behind all these components. The correction plane is located behind the amplitude, phase and polarization modulation (APP-modulation).
In the image plane, the polarization measurement of modulated beams is performed with the help of an additional, rotatable QWP and a polarizer (Pol.) [23]. Consequently, the correction for the polarization modulation is calculated for the image plane according to the procedure described in section 3.2.

4.2 Realization of Poincaré beams

If the correction methods are implemented, different Poincaré beams with spatially varying states of polarization in their transverse plane can be created accurately as depicted in figure 7 and in section 4.3, figure 8. Figure 7 shows two examples of beams modulated in amplitude, phase and polarization: a) illustrates the accessibl states of polarization for the used settings of $\beta_1 = -45°$ and $\beta_2 = 90°$ for the two QWPs of the SPM. b) and c) demonstrate two even Laguerre-Gaussian beams ($LG^e_{5,3}$), while in b) every intensity ring of the LG beam and in c) each intensity spot got its own state of polarization. The Stokes parameters can be determined in each camera pixel by the help of the rotatable QWP and fixed polarizer [23], while the measured polarization of every fifth pixel is depicted by small, calculated polarization ellipses drawn upon the measured intensity image of the beam; red ellipses indicate right elliptical, blue left elliptical and green linear states of polarization, respectively. The holograms used for the polarization modulation ($\Delta\phi_{SLM}$, without correction pattern) are shown for both beams. Additionally, in b) the measured Stokes parameters are depicted and in c) the determined opening angle ($\tan(\chi)$) of the polarization ellipses is represented. The measured parameters clarify the efficiency of the modulation method – the full combination of amplitude, phase, and polarization modulation of the complete transverse plane is realized very precisely.

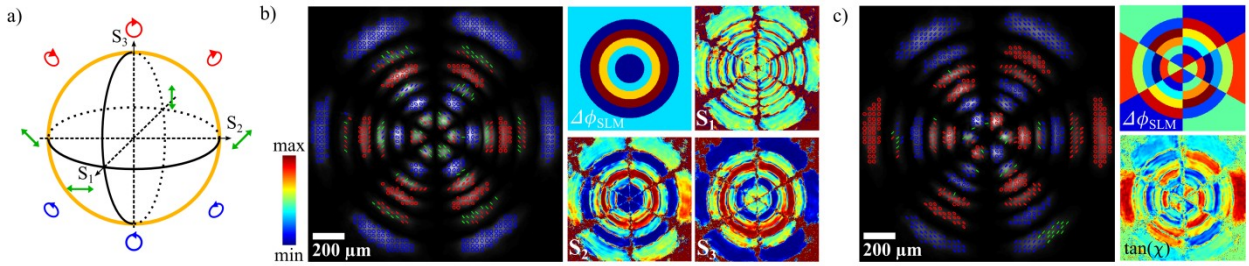

Figure 7. Poincaré beams: even Laguerre-Gaussian beams ($LG^e_{5,3}$) with spatially varying states of polarization. The reachable states of polarization for the used setting $\beta_1 = -45°$ and $\beta_2 = 90°$ are depicted on the Poincaré sphere in a). b) shows the measured transverse plane of a Laguerre-Gaussian beam, while each intensity ring has its own state of polarization (red/ blue: right/ left elliptical states of polarization, green: linear states of polarization). The $LG^e_{5,3}$-beam is generated by the first half of the SLM (amplitude and phase modulation), while the SPM creates the desired distribution of polarization by the use of the phase hologram $\Delta\phi_{SLM}$ ($\min = 0$, $\max = 2\pi$) illustrated in the subfigure. The measured Stokes parameters S_1, S_2 and S_3 ($\min = -1$, $\max = 1$) match the modulated ring structure. Subfigure c) also shows a modulated $LG^e_{5,3}$-beam, while in this case each intensity spot in the transverse plane has its own state of polarization as additionally visible in the corresponding polarization modulation hologram $\Delta\phi_{SLM}$ and the measured opening angle of polarization ellipses ($\tan(\chi)$; $\min = -1$, $\max = 1$).

4.3 Polarization singularities in the transverse plane of Poincaré beams

Scalar singularities in the form of phase vortices have attracted considerable interest for already many years [24]. Compared to this, vectorial singularities as polarization singularities form a young research area enjoying no less interest than scalar singularities [3]. With our described setup we are not only able to combine complex light fields as Laguerre-Gaussian beams with spatially varying polarization structures as shown in figure 7, but also to generate vectorial singularities as V-Points, L-Lines and C-Lines [3] in the transverse plane of Poincaré beams. For this purpose, the incoming light field is not modulated in amplitude and phase by the first half of the SLM. It is only the phase correction pattern that is implemented in this part in such way that that the beam is solely modulated with respect to its polarization by the SPM. By a suitable choice of the polarization modulation pattern $\Delta\phi_{SLM}$ and superimposed correction pattern δ_{corr} polarization singularities in elliptic polarization fields [4] with spatially continuously changing polarization can be created efficiently.

Figure 8 demonstrates this additional possibility of modulating polarization singularities. For the shown experimental results, the QWPs' angles are again fixed at $\beta_1 = -45°$ and $\beta_2 = 90°$, so that all reachable polarization states can be found on the ring in the S_2-S_3-plane on the Poincaré sphere (see fig. 7 a)).

Figure 8 a) - c) show three different types of modulated beams with a continuously changing polarization structure including all three singularities. Depending on the modulation pattern, a desired number of singularities at chosen

positions can be created. Each subfigure includes the measured polarization ellipses depicted upon the intensity image, the opening angle of polarization ellipses ($\tan(\chi)$) and a sketch of polarization singularities located in the transverse plane of the beam (black: V-Point, red/ blue: right/ left circular polarized C-Line, green: linear polarized L-Line).

In contrast to figure 8 a) - c), figure 8 d) - f) only include line singularities as L-Lines and C-Lines. They form closed paths in the transverse plane of the beam, while different shapes are achieved as circular and elliptical rings (d) + e)) or even more complex shapes as shown in figure f). Again, the opening angle of the polarization ellipses and the sketch of included polarization singularities are shown.

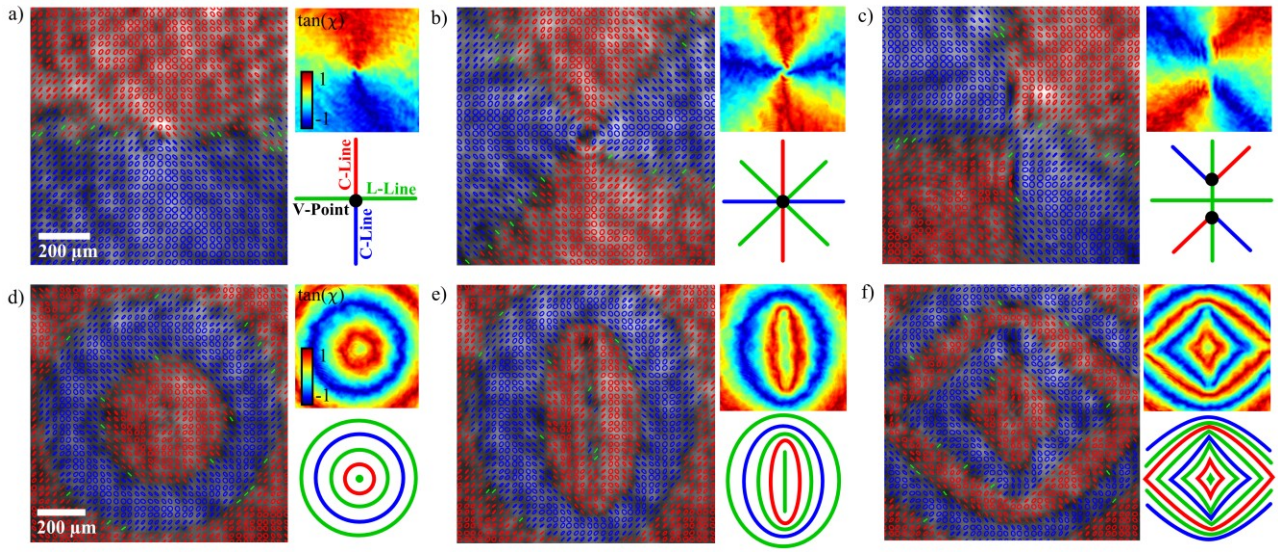

Figure 8. Polarization singularities in the transverse plane of Poincaré beams: Each shown beam contains a continuous change in polarization along the regarded transverse plane (see $\tan(\chi)$), while the beams are generated without amplitude and phase modulation by the first half of the SLM. Subfigure a) to c) depicts Poincaré beams including L- and C-Line singularities in its flowing structure ending in a V-Point singularity, where, as expected, the absence of intensity is caused. The included singularities are visualized by a sketch, where blue/ red lines symbolize left/ right circular polarized line singularities (C-Lines), green lines indicates linear polarized lines singularities (L-Lines), V-Points are shown in black. Subfigure d) - f) illustrate Poincaré beams without V-Points, but with L- and C-Line singularities. In this case, the line singularities form closed paths as obviously in the lines sketches.

To summarize, our holographic setup is not only capable of tailoring complex light fields by amplitude and phase modulation but also allows arbitrarily modulating the states of polarization such that Poincaré beams even with polarization singularities can be created. Different kinds of Poincaré beams are possible: complex light fields modulated discretely in polarization, that means discrete areas of the beam are chosen to have the same state of polarization, or light fields modulated with continuously varying polarization. In continuously varying polarization structures polarization singularities can occur. Amount, position and kind of polarization singularities in the transverse plane of the Poincaré beam can be chosen, so that the form of line singularities can be influenced arbitrarily and e.g. closed paths as shown in figure 8 d) - f) become possible.

5. CONCLUSION

We demonstrated the ability of our holographic method to modulate amplitude, phase and polarization by using a phase-only SLM as a main component. We fully combined these three aspects by modulating the beam's complete transverse plane (section 4). In section 2, we have shown the effective modulation of amplitude and phase by the example of higher order Laguerre-Gaussian beams, while section 3 introduced the possibility of modulating spatially varying states of polarization with the help of the SPM – a modulation system consisting of two quarter wave plates and a SLM. In order to combine amplitude, phase and polarization modulation the used SLM operates in split-screen-mode. To enhance the

quality of modulation several correction methods regarding phase and amplitude as well as polarization modulation have been introduced, whose application results in efficiently modulated Poincaré beams.
We have shown different experimental results regarding the combination of amplitude, phase and polarization modulation: higher order Laguerre-Gaussian beams with different discrete polarization structures were created. Finally, we realized the generation of polarization singularities in the transverse plane of Poincaré beams. Our method even allows their arbitrary transverse location in fields of continuously varying states of polarization. V-Points, C-Lines and L-Lines were shown, while their amount is variable. Moreover, line singularities' form can be influenced so that even closed paths could be modulated holographically in the beams' transverse plane.

Consequently, the described holographic setup allows the application and investigation of arbitrary kinds of polarization singularities and, moreover, of beams modulated in amplitude, phase and polarization simultaneously. Our results give rise to promising applications in optical micromanipulation and advanced information encoding, where the shown correction methods are beneficial in order to achieve efficiently modulated beams.

ACKNOWLEDGEMENT

This work was partially supported by the German Research foundation (DFG) in the frame of Cells-in-Motion Cluster of Excellence (EXC 1003 – CiM) and the German-Chinese transregional research project TRR61 both University of Muenster, Germany.

REFERENCES

[1] Brown, T. G., [Unconventional Polarization States: Beam Propagation, Focusing, and Imaging], Progress in Optics 56, Elsevier, 81-129 (2011)
[2] Beckley, A.M., Brown, T. G. and Alonso, M. A., "Full Poincaré beams", Opt. Express 18, OSA, 10777-10785 (2010)
[3] Dennis, M. R., O'Holleran, K. and Padgett, M. J., [Singular Optics: Optical Vortices and Polarization Singularities], Progress in Optics 53, Elsevier, 293-363 (2009)
[4] Freund, I., "Polarization singularity indices in Gaussian laser beams", Optics Communications 201, 251-270 (2002)
[5] Quabis, S., Dorn, R. and Leuchs, G., "Generation of a radially polarized doughnut mode of high quality", Applied Physics B 81, 597-600 (2005)
[6] Cardano, F., Karimi, E., Slussarenko, S., Marrucci, L., de Lisio, C. and Santamato, E., "Polarization pattern of vector vortex beams generated by q-plates with different topological charges", Appl. Opt. 51(10), OSA, C1-C6 (2012)
[7] Galvez, E. J., Khadka, S., Schubert, W. H. and Nomoto, S., "Poincaré-beam patterns produced by nonseparable superposition of Laguerre-Gauss and polarization modes of light", Appl. Opt. 51(15), OSA, 2925-2934 (2012)
[8] Woerdemann, M., Alpmann, C., Esseling, M., and Denz, C., "Advanced optical trapping by complex beam shaping", Laser & Photonics Reviews 7, 839-854 (2013)
[9] Andrews, D. L., [Structured light and its applications: An introduction to phase-structured beams and nanoscale optical forces], Academic Press (2011)
[10] Seunarine, K., Calton, D., Underwood, I., Stevenson, J., Gundlach, A. and Begbie, M., "Techniques to improve the flatness of reflective micro-optical arrays", Sensors and Actuators A: Physical 78(1), 18-27 (1999)
[11] Matrin-Badosa, E., Montes-Usategui, M., Carnicer, A., Andilla, J., Pleguezuelos, E. and Juvells, I., "Design strategies for optimizing holographic optical tweezers set-ups", Journal of Optics A 9(8), S267-S277 (2007)
[12] Wulff, K. D., Cole, D. G., Clark, R. L., DiLeonardo, R., Leach, J., Cooper, J., Gibson, G. and Padgett, M. J., "Aberration correction in holographic optical tweezers", Opt. Express 14(9), OSA, 4169-4174 (2006)
[13] Cižmár, T., Mazilu, M. and Kishan, D., "In situ wavefront correction and its application to micromanipulation", Nature Photonics 4 (2010)
[14] Friese, M., Nieminen, T., Heckenberg, N. and Rubinsztein-Dunlop, H., "Optical alignment and spinning of laser-trapped microscopic particles" Nature 394(6691), 348-350 (1998)

[15] Mair, A., Vaziri, A., Weihs, G. and Zellinger, A., “Entanglement of the orbital angular momentum states of photons”, Nature 412(6844), 313 (2001)
[16] Gibson, G., Courtial, J., Padgett, M., Vasnetsov, M., Pas'ko, V., Barnett, S. and Franke-Arnold, S., “Free-space information transfer using light beams carrying orbital angular momentum”, Opt. Express 12(22), OSA, 5448-5456 (2004)
[17] Davis, J., Cottrell, D. Campos, J., Yzuel, M. and Moreno, I., “Encoding amplitude information onto phase-only filters”, Appl. Opt. 38(23), 5004-5013 (1999)
[18] Goodman, J., [Introduction to Fourier optics], McGraw-Hill (2008)
[19] Alpmann, C., Boguslawski, M., Rose, P. and Woerdemann, M., “Tailored light fields: nondiffracting and self-similar beams for optical structuring and organization”, Proc. SPIE 8274, 82740R1-12 (2012)
[20] Yoshiki, K., Hashimoto, M. and Araki, T., “Second-harmonic-generation microscopy using excitation beam with controlled polarization pattern to determine three-dimensional molecular orientation”, Japanese Journal of Applied Physics 44(34), L1066-L1068 (2005)
[21] Alpmann, C., Schlickriede, C., Otte, E. and Denz, C., “Dynamic modulation of Poincaré beams”, submitted
[22] Han, W., Yang, Y., Cheng, W. and Zhan, Q., “Vectorial optical field generator for the creation of arbitrarily complex fields”, Opt. Express 21(17), OSA, 20692-20706 (2013)
[23] Schaefer, B., Collett, E., Smyth, R., Barrett, D. and Fraher, B., “Measuring the Stokes polarization parameters”, American Journal of Physics 75(2), 163-168 (2007)
[24] Soskin, M. and Vasnetsov, M., [Singular optics], Progress in optics 42(4), Amsterdam: North-Holland Pub. Co., 219-276 (2001)